The Journal of Experimental Biology 206, 2441-2457

doi:10.1242/jeb.00433

Food transport in the *C. elegans* pharynx

Leon Avery* and Boris B. Shtonda

Department of Molecular Biology, University of Texas Southwestern Medical Center, 5323 Harry Hines Boulevard, Dallas, Texas 75390-9148, USA

*Author for correspondence (e-mail: leon@eatworms.swmed.edu)

Accepted 3 April 2003

Summary

Pumping of the *C. elegans* pharynx transports food particles (bacteria) posteriorly. We examined muscle motions to determine how this posterior transport is effected. We find that the motions of the middle section of the pharynx, the anterior isthmus, are delayed relative to the anterior section, the corpus. Simulations in which particles are assumed to move at mean fluid velocity when not captured by the walls of the pharyngeal lumen show that delayed isthmus motions do indeed cause net particle transport; however, the amount is much less than in the real pharynx. We propose that the geometry of the pharyngeal lumen forces particles to the center, where they move faster than mean fluid velocity. When this acceleration is incorporated into the simulation, particles are transported efficiently. The transport mechanism we propose explains past observations that the timing of muscle relaxation is important for effective transport. Our model also makes a prediction, which we confirm, that smaller bacteria are better food sources for *C. elegans* than large ones.

Key words: nematode, *Caenorhabditis elegans*, pharynx, food transport, hydrodynamic simulation, feeding.

Introduction

Like many soil nematodes, *Caenorhabditis elegans* feeds on bacteria suspended in liquid. Bacteria are transported from the mouth to the intestine by a neuromuscular tube called the pharynx. The pharynx functions as a pump, generating pressure to force food into the intestine, necessary because the interior of the nematode is at higher pressure than the surrounding environment (Harris and Crofton, 1957). The pharynx, however, is more than just a pump; it also concentrates food. Bacteria are trapped and transported posteriorly along the pharyngeal lumen, but most of the liquid in which they are suspended is expelled through the mouth, rather than being pumped into the intestine. This concentration of food particles is presumably important for efficient digestion and absorption. The volume of the intestinal lumen is limited, and a small ingested volume allows food to reside in the intestine longer. [Ingested materials spend an astonishingly short time in the intestine: tracers such as mineral oil or latex beads pass through the intestine of a rapidly feeding adult in 3–10 min (L. Avery, unpublished data)]. The smaller ingested food volume would also concentrate nutrients, allowing them to be more efficiently absorbed, and reduce the dilution of any digestive enzymes. Concentration of particles by the pharynx does not depend on their specific chemical properties, since 0.9 μm carboxylated latex beads are also efficiently concentrated (L. Avery, unpublished data).

C. elegans is, therefore, a filter feeder. It takes in liquid with suspended food particles, traps the particles, and expels the liquid. However, unlike many filter feeders, which separate food from medium by passing the suspension through a mesh that traps the food particles, there is no obvious filter in the pharynx through which particles and liquid are separated. A striking example of differential motion of particles and fluid is posteriorward transport of particles within the anterior half of the pharynx, the corpus (Fig. 1). During active feeding, bacteria are found at various points along the length of the relaxed corpus. Corpus muscles contract when a feeding motion (a pump) begins, and fluid rushes in at the mouth, sweeping food particles posteriorly. The contraction is followed by relaxation, which closes the lumen and expels the fluid. Unlike the fluid, the bacteria do not return to their original positions; when the motion is finished, they are seen to be located more posteriorly than they were before it started. This posteriorward transport is of course essential for the function of the pharynx, moving food from the mouth to the intestine.

In our attempts to understand feeding *C. elegans*, we have identified many defects, either genetic mutations or laser killing of pharyngeal neurons, that result in inefficient feeding. Most of these fall into two categories. In the first category are all those defects that decrease the *rate* of feeding. Most or all of these defects affect the excitatory motor neuron MC (Raizen et al., 1995). It is obvious why worms that fail to excite pharyngeal muscle pump slowly, and why slow pumping causes inefficient feeding. The second category contains

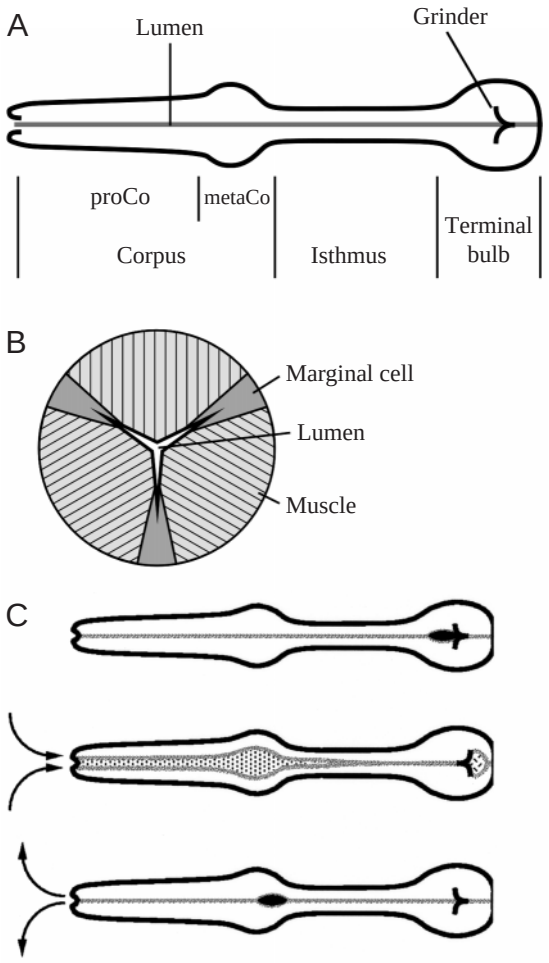

Fig. 1. Pharyngeal anatomy and pharyngeal pumping. (A) The pharynx is a tubular muscle divided into three regions: the corpus, connected to the mouth at the anterior end, the isthmus, and the terminal bulb, connected to the intestine at the posterior end. The corpus is further subdivided into a cylindrical or tapered anterior section, the procorpus (proCo), and a posterior bulb, the metacorpus (metaCo). (B) Simplified schematic cross-section through the pharynx. The lumen is shown almost closed, and is approximately to scale. The hatching in the muscle cells shows the orientation of their acto-myosin filaments. When they contract the muscle cells become thinner in the radial dimension and longer circumferentially, pulling the lumen open. Three intermediate filament-containing marginal cells anchor the apices of the lumen. (C) Pharyngeal pumping is a contraction–relaxation cycle involving the corpus, anterior half of the isthmus and terminal bulb. The cycle begins with the near-simultaneous contraction of these muscles. Contraction of the radially oriented muscles of the corpus and anterior isthmus opens the lumen. Because the posterior isthmus remains closed during this time, the lumen is filled by liquid sucked in through the mouth, carrying with it suspended food particles. Contraction of the terminal bulb rotates the plates of the grinder, breaking bacteria in the terminal bulb and passing the debris back to the intestine. After contraction there is a near-simultaneous relaxation, returning the grinder to its resting position and closing the lumen of the corpus and anterior isthmus. Liquid is expelled from the corpus and anterior isthmus, but food particles are trapped and transported posteriorly. A second motion of the pharyngeal muscles, posterior isthmus peristalsis (not shown here) carries food from the anterior isthmus back to the terminal bulb.

defects that affect *transport* of food in the corpus. In laser killing experiments, the inhibitory motor neuron M3, which controls the timing of pharyngeal muscle relaxation, is often a key component of these defects (Avery, 1993b). Genetically, transport defects result either from defects in M3 function (Dent et al., 1997; Lee et al., 1999) or G protein signaling (see for example, Robatzek et al., 2001), which probably also affects relaxation timing (Niacaris and Avery, 2002). It is not obvious how these defects in relaxation timing cause poor transport. To understand the genetics of feeding, it has therefore become necessary to understand how the pharynx transports food.

Transport of bacteria within the corpus is puzzling, because the motions of the corpus muscles during relaxation appear to be the reverse of the motions during contraction. One might imagine that particles could be retained by inertia during relaxation; heavy particles, slow to start moving, would lag behind the liquid. However, in a system as small as the *C. elegans* pharynx, fluid motions should be dominated by viscous (frictional) forces, and inertial forces should be negligible. In systems of such low Reynolds number (the ratio of inertial to viscous forces), motions are reversible and linearly related to force (Vogel, 1994). Consequently, a reciprocal motion has no net effect (Purcell, 1977). The pharynx should not work.

In this paper we show by analysis of videotapes that the motions of the anterior pharyngeal muscles during relaxation are not precisely the reverse of those during contraction. Corpus motions may be purely reciprocal, but the motions of the isthmus muscles immediately posterior to the corpus are slightly delayed, so that the isthmus is relaxed when the corpus begins to contract but contracted when the corpus relaxes. Simulation shows that this small deviation from perfectly reciprocal motion is sufficient to produce a small degree of net posteriorward particle transport if the particles are assumed to move at the same average speed as the fluid. However, transport is much less efficient in this simulation than in the animal. To resolve this discrepancy, we propose that the geometry of the pharyngeal lumen causes particles to be pushed to the center of the pharyngeal lumen during relaxation. Because fluid velocity is fastest at the center of a tube, the bacteria move faster than the mean fluid velocity. When this assumption is incorporated into the simulation, transport becomes efficient. The transport mechanism can be understood in simple, intuitive terms. In addition, this model explains why the genetic and microsurgical perturbations described above result in inefficient transport, and makes a prediction, which we confirm, that small bacteria will be better food than large bacteria.

Materials and methods

Video recordings and analysis

Video recordings were made from either wild-type (strain

Table 1. *Pharyngeal dimensions in* C. elegans

A. Lengths (μm)

		Pharynx				
	Worm	Corpus	Isthmus	Terminal bulb	Total	Pharynx/worm (%)
Adults	1002.2±28.3*	76.6±0.8	35.8±0.9	32.3±0.5	144.7±0.9	14.4±0.4
L1s	241.6±10.0*	35.0±0.7	23.6±0.5	13.0±0.3	71.6±1.0	29.6±1.3

B. Diameters (μm)

				Procorpus	
	Terminal bulb	Isthmus	Metacorpus	Posterior	Anterior
Adults	31.5±1.1	15.3±0.3	27.1±0.5	19.2±0.3	15.1±0.2
L1s	9.6±0.1	4.0±0.1	8.6±0.2	6.7±0.1	6.1±0.1

C. Estimated lumen diameters (μm)

	Isthmus	Procorpus
Adults	3.9	4.9
L1s	1.0	1.8

Values are means ± S.E.M.
N=6 in A (**N*=4 for the whole worm length measurements); *N*=10 in B.
L1s, first stage larvae.

N2) or *unc-29(e1072)* (strain CB1072) *Caenorhabditis elegans* worms, mounted on agar pads and observed with differential interference contrast optics according to standard methods (Sulston and Hodgkin, 1988). Recordings were digitized with a Pinnacle DV500 video capture board, either direct from a microscope-mounted grayscale camera or from S-VHS video recordings. MPEG2 format video files were split into frames (1/30 s apart), then the odd and even lines of each frame were separated into fields (1/60 s apart) as described previously (Avery, 1993a).

Pharyngeal dimensions

To measure the outer dimensions of the pharynx, worms were mounted on pads of 4% agar in M9 buffer (Sulston and Hodgkin, 1988) containing 50 mmol l^{-1} sodium azide to immobilize them, and measurements were taken from animals that were lying straight or nearly straight. Six gravid adult hermaphrodites and ten first-stage larvae (L1) mounting within 1 h and 11 min of hatching were measured with an ocular micrometer, calibrated with a stage micrometer. The results are shown in Table 1.

To estimate lumen dimensions, we measured electron micrographs published by Albertson and Thomson (1976). For instance, fig. 5 of that paper is a cross-section of the procorpus. The diameter of the procorpus in that figure is 14.8 cm. Since the actual mean diameter of the adult procorpus is 17.1 μm (Table 1B), the printed electron micrograph is magnified 8600 times. The mean distance from the center of the pharynx to the apices of the three radii of the relaxed pharynx in the figure is 3.7 cm, which corresponds to 4.2 μm in the adult procorpus. Assuming that the cuticle lining the pharyngeal lumen does not shrink or stretch, the perimeter of the lumen is six times this, or 25 μm. Finally, if the lumen cross-section is assumed to have the shape of an equilateral triangle when fully open, its maximum diameter (defined as the diameter of an inscribed circle) is the perimeter divided by $3\sqrt{3}$, or 4.9 μm. Similar measurements of fig. 6 of Albertson and Thomson (1976), a section through the isthmus, and application of the same calculations to the adult isthmus and to the L1 isthmus and procorpus (assuming that the ratio of lumen diameter to pharynx outer diameter is the same in L1s as in adults) give rise to the estimates in Table 1C. While there are several unverified assumptions in these calculations, they are likely to be more accurate than can be made directly from video recordings of the contracted pharynx, and they are broadly consistent with other observations. For instance, 0.8 μm latex beads fit in the isthmus with little room to spare, consistent with the calculated 1.0 μm diameter, and adults can swallow 4–5 μm iron particles (Avery and Horvitz, 1990), but only with difficulty, consistent with the estimated 3.9 μm diameter of the isthmus, assuming that pressure from the corpus can force the isthmus lumen to open slightly beyond a triangular cross-section. (If the isthmus opened to a circular cross-section, a particle up to 6.4 μm in diameter could be accommodated without cuticle stretching.)

To estimate how lumen diameter varied along the length of the pharynx, an image of the pharynx was imported into a vector drawing program (Deneba Canvas) and a curve was drawn on it representing the approximate shape of the open lumen remembered from video recordings. (We could not draw direct from video images because the pharynx is never straight, in focus, and immobile enough to image sharply along the

entire length of the anterior isthmus and corpus.) The procorpus and isthmus were drawn as constant in diameter along their lengths, and the metacorpus was represented by an elliptical section. The drawn shape was converted into a bitmap and diameters read from the resulting file. Finally, the dimensions were adjusted to match the measurements and estimates in Table 1A and C. In the simulations an L1 size pharynx transports 0.7 μm diameter particles (estimated size of a typical *E. coli* cell, based on comparison with 0.8 μm latex beads).

Isolation, identification, and photography of soil bacteria

Soil samples collected in five locations in the Dallas metroplex area were suspended in water and plated at different dilutions on LB plates until single bacterial colonies could be identified. Colonies that appeared homogeneous, fast growing and different from each other were replated 2–3 times until clean cultures were obtained. Identification of bacteria was done by commercial 16S rDNA sequencing (Midilabs, 125 Sandy Drive Newark, DE 19713, USA; www.midilabs.com), and sequences were aligned against the provider's MicroSeq database. According to the provider's recommendations, strains with less than 1% sequence differences from the best database match were considered a species match, strains with 1–3% difference from the closest match were considered a genus match, isolates with >3% difference were considered not to match. For photography, we removed bacteria from an NGM or NGMSR plate (identical to the plates on which growth rate measurements were made) with a platinum wire and transferred them to pads of 3% agarose in M9 salts, added a small amount of a suspension of 0.8 μm blue-dyed latex beads (Sigma stock number L1398) and a coverslip, and photographed them on Kodak elite chrome 200 slide film under differential interference contrast optics.

Growth rate measurements

Growth rate was defined as an inverse of the number of days taken for an animal to grow from the L1 stage to adulthood. Plates for growth rate measurements were prepared as follows. Bacteria were grown for 1 or 2 days on 60 mm NGM plates to obtain a bacterial lawn covering approximately 50% of the plate area. For most of our work, worms were grown on lawns of *E. coli* HB101 or DA837 on NGMSR medium, which contains streptomycin and nystatin to reduce growth of contaminants (Davis et al., 1995). We also used NGMSR for the measurement of growth rates on HB101 and DA837. Growth rate measurements on the soil bacteria isolates were done instead on NGM (Sulston and Hodgkin, 1988), since the soil bacteria isolates were sensitive to streptomycin. 50–100 starved synchronized L1s were transferred to a plate, which thereafter was kept at 18°C and observed every 1–3 h until approximately 50% of the animals reached the adult stage. The inverse of time (in days) it took hermaphrodites to become adults was plotted as growth rate. Adults were recognized by the appearance of a mature vulva, and by the production after several hours of eggs. The error bars extend from the inverse of the time of the first observation after that at which worms reached the adult stage to the inverse of the time of the last observation before that at which worms reached the adult stage. Worms were synchronized by egg starvation (Emmons et al., 1979): virgin adult hermaphrodites were lysed in 40% bleach, 0.5 mol l^{-1} sodium hydroxide for 5 min followed by three washes in M9, then eggs were incubated overnight in M9 at 18°C to allow L1s to hatch.

Results

Overview of pharyngeal pumping

The pharynx of *Caenorhabditis elegans* is divided into three anatomical regions: the corpus, the isthmus, and the terminal bulb (Fig. 1). During normal feeding, the pharynx executes two motions: pumping and isthmus peristalsis (Avery and Horvitz, 1989). A pump consists of a near-simultaneous contraction of the muscles of the corpus, anterior isthmus and terminal bulb, followed by a near-simultaneous relaxation. Contraction and relaxation of the corpus and anterior isthmus result in accumulation of food in the lumen, as described below. Contraction of the terminal bulb inverts the plates of the grinder, breaking up any bacteria that were in front of the grinder at the start of the pump and passing them back to the intestine. The posterior isthmus remains closed during pumping, so that the anterior isthmus and corpus are hydrodynamically isolated from the terminal bulb. The second motion of the pharynx, isthmus peristalsis, occurs after approximately every fourth pump and carries food from the anterior isthmus to the terminal bulb (Avery and Horvitz, 1987).

This paper is concerned with transport of food by the corpus and anterior isthmus during pumping. Transport is one of two functions of the corpus and anterior isthmus, the other being trapping. The muscles of the corpus and isthmus are radially oriented, so that when they contract, the lumen opens. When the lumen of the corpus and anterior isthmus opens, it is filled by liquid sucked in through the mouth. Suspended bacteria are carried in with the liquid. Relaxation closes the lumen of the pharynx, expelling the liquid. Some or all of the bacteria, however, remain in the pharynx. This is trapping. At the beginning of the next pump, the previously trapped bacteria are found in the lumen of the pharynx. When the muscles contract, the bacteria are carried posteriorly by the inflow of liquid. They do not return to their original position when the muscle relaxes, however; after relaxation they are found at a more posterior position than they occupied before contraction. With repeated pumps all food is carried back to the isthmus (Avery, 1993b). This is transport. Unfortunately, it is difficult to see by simple observation how transport works. The relaxation is very rapid: the corpus usually goes from fully open to closed in less than 1/60 of a second, the smallest time interval that can be resolved in a standard NTSC video. It has therefore not been possible to watch particle motion during relaxation.

Motions of beads during pumping

In an attempt to record the motions of particles during

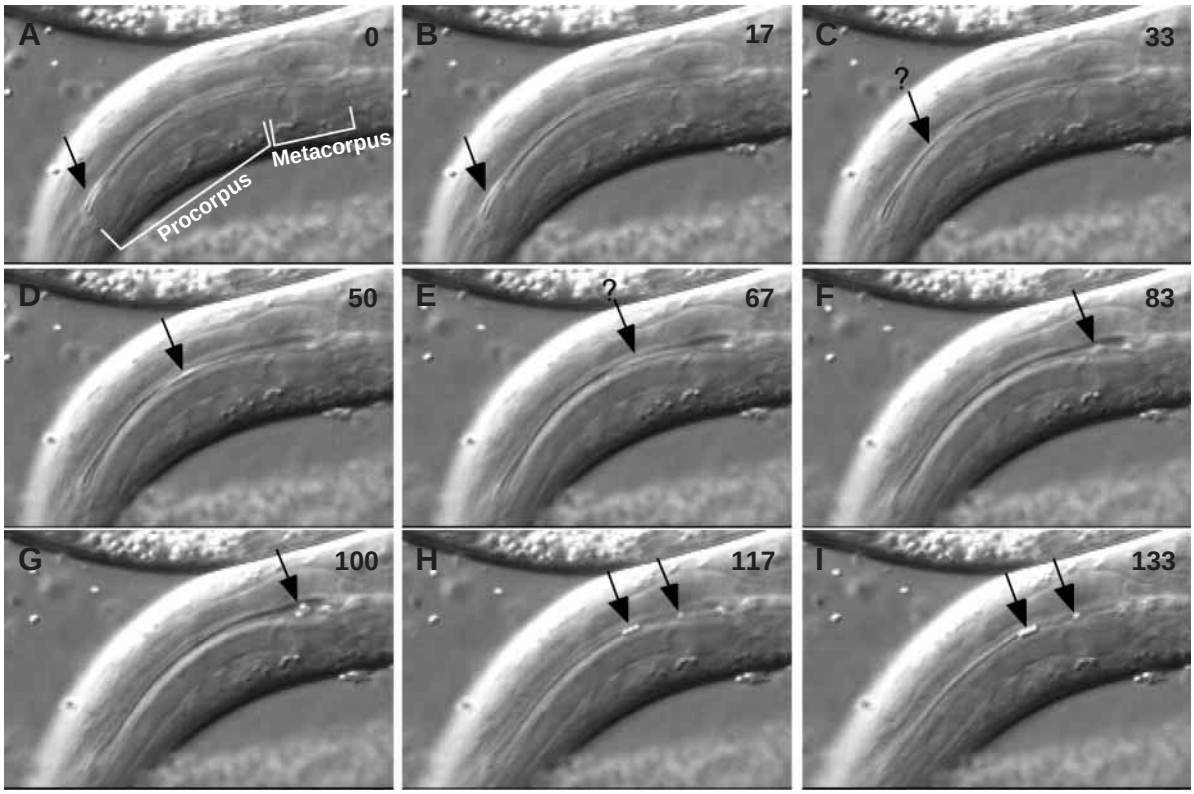

Fig. 2. Particle motions. This sequence of consecutive video fields shows the transport of 3 or 4 latex beads from the anterior end of the procorpus to the posterior procorpus or metacorpus. Time in ms is shown in the upper right corner of each image. (A) At time 0 the pharynx is relaxed (lumen closed) and the particles (black arrow), slightly out of focus but detectable by their refractility, are lined up in the anterior procorpus. (B) The contraction has begun (visible as a slight expansion of the procorpus lumen), but the particles have not moved. (C–G) Contraction progresses and the particles are drawn back to the metacorpus. The black arrow indicates the particles. They are not clearly visible in C and E, probably because they are out of focus or moving too rapidly or both; here the black arrow is a guess at their location. Between G and H the corpus muscles partly relaxed and the particles moved forward, three to the posterior procorpus and one to anterior metacorpus. (We do not know whether this fourth particle was at the anterior procorpus at time 0, or out of focus at a more posterior position.) (I) Relaxation is complete. The beads do not move between H and I.

pumping, we fed worms blue-dyed 0.8 μm latex beads, hoping that since they are high-contrast objects under differential interference contrast, dyed beads would be easier to see during rapid motion than bacteria. This experiment was mostly unsuccessful; however, one useful sequence, shown in Fig. 2, was found in several minutes of recording. The sequence began with the corpus fully relaxed and 3 or 4 beads at its anterior end (Fig. 2A). 17 ms later the corpus had begun to contract, but the particles had not moved. During the next 83 ms (Fig. 2C–G) the contraction of the corpus continued, and the beads moved from the anterior end of the corpus to the lumen of the metacorpus. In the next field (Fig. 2H) the relaxation was in progress. One bead had moved forward to the anterior metacorpus, and three to the posterior procorpus. In the final field (Fig. 2I) the relaxation was complete. The beads did not move in the final 17 ms.

This sequence demonstrates net posteriorward particle transport. The beads began in the anterior corpus and finished in the posterior corpus, although they moved both posteriorly and anteriorly during the pump. It also shows that particles do not always move with fluid in the pharyngeal lumen. This is most obvious in Fig. 2H,I. During this interval the corpus went from partially contracted to fully relaxed, and the liquid filling the metacorpus must have flowed anteriorly through the procorpus to the mouth. However, the four latex beads in the posterior procorpus and anterior metacorpus did not move.

Anterior isthmus motions are delayed

At low temporal resolution, the corpus and anterior isthmus appear to undergo a simple reciprocal motion during pumping, in which the relaxation is just the reverse of the contraction. As argued above, such a reciprocal motion cannot easily explain net transport of food particles. We therefore examined the motions of the corpus and isthmus using videotapes.

Within the resolution of this analysis, motions of the corpus were simultaneous along its entire length. However, as demonstrated in Fig. 3, the motions of the anterior isthmus were slightly delayed relative to the corpus. In this series, the first visible contraction of the corpus was seen at 33 ms. The isthmus was still closed at 100 ms; its first visible opening occurred in

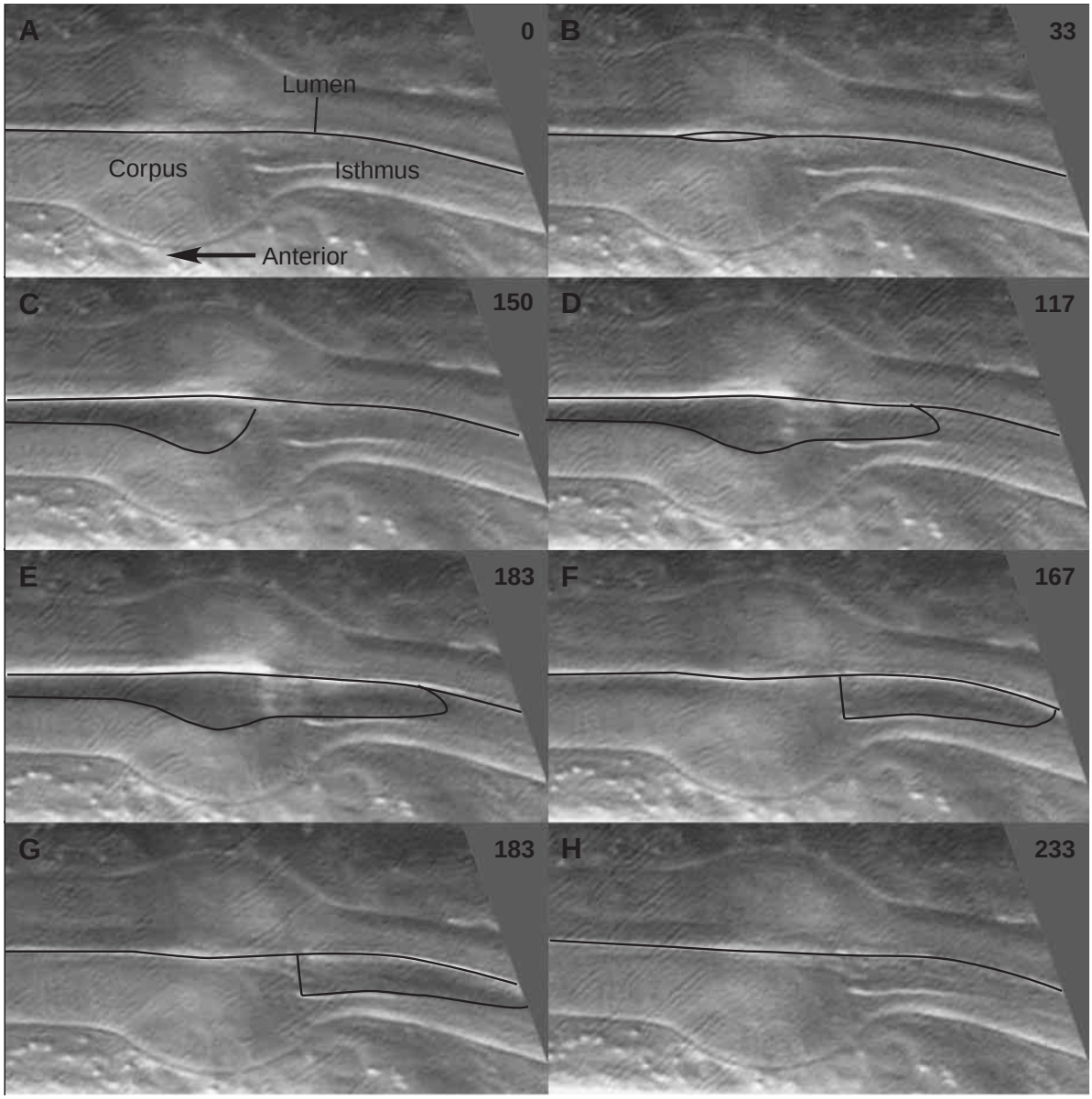

Fig. 3. Anterior isthmus motions. Non-consecutive series of video fields shows the motions of the metacorpus and anterior isthmus during a pump. Black lines show the lumen; time in ms is in the upper right corner of each image.(A) The pharynx is fully relaxed, the lumen closed. At 33 ms (B) contraction (opening) of the metacorpus is barely visible, and at 100 ms (C) contraction is complete and the corpus lumen fully open. Only at 117 ms (D), after the corpus has fully contracted, does the anteriormost part of the isthmus open. The metacorpus remains fully contracted until 150 ms (E), then goes from fully open to fully closed between two consecutive video fields at 150 and 167 ms (F). In the meantime the isthmus contraction proceeds, gradually opening more posteriorly until at 183 ms (G) the entire anterior half of the isthmus is open. At 233 ms (H) the isthmus is fully relaxed.

the next field, at 117 ms. Similarly, while the corpus went from fully contracted to relaxed between 150 and 167 ms, the anterior isthmus did not relax until 233 ms. Furthermore, the anterior isthmus did not contract simultaneously along its length. At 117 ms, only the anteriormost part of the isthmus was open. In the following frames, the opening extended progressively more posteriorly, as can be seen in the fields at 150, 167 and 183 ms. Thus, unlike the corpus, which contracted and relaxed as a unit, the anterior isthmus contracted in a wave that swept rapidly from anterior to posterior.

The precise timing of pharyngeal muscle motions is variable. Table 2 shows the delay of isthmus motions with respect to corpus motions in two animals. Neither of these is the animal of Fig. 3. The duration of the corpus contraction typically varies between 100 ms and 1 s. However, the features described above and demonstrated in Fig. 3 were consistent: corpus motions were simultaneous, but anterior isthmus motions were delayed with respect to the corpus, and both the opening and the closing of the anterior half of the isthmus began at the anterior end and progressed posteriorly to the

Table 2. *Isthmus delay*

	Contraction delay (ms)			Relaxation delay (ms)		
Worm	Mean	Range	*N*	Mean	Range	*N*
1	43±8	17–67	5	27±7	17–50	5
2	40±8	17–117	14	46±5	17–83	12

Measurements from two worms of the delay of isthmus motions relative to corpus motions.

Contraction delay is the delay between the first visible metacorpus contraction and the first visible anterior isthmus contraction in a pump.

Relaxation delay is defined analogously.

Values are means ± S.E.M.

middle. Because of the anterior isthmus motions, pharyngeal muscle motions during corpus relaxation were not the reverse of motions during contraction. For instance, the isthmus was closed during most of the corpus contraction, but was contracting while the corpus relaxed.

Simulation of particle transport

To find out whether the delayed motions of the isthmus could account for transport of particles in the corpus, we simulated the motions of fluid and particles in the pharyngeal lumen. Particles were assumed to move according to two rules. (1) When the diameter of the pharyngeal lumen (defined as the diameter of an inscribed circle) is the same as or smaller than the particle diameter, the particle is held by the walls of the lumen and unable to move (Fig. 4). (2) When the diameter of the pharyngeal lumen is greater than the particle diameter, particles are free to move, and move with the fluid.

Interaction between particles was not modeled, so the simulation is strictly valid only for a nearly empty pharynx.

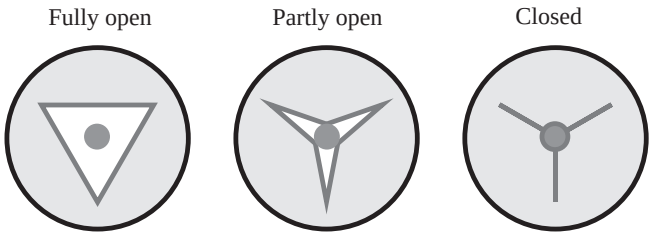

Fig. 4. Particle trapping by the walls of the pharyngeal lumen. The pharyngeal lumen has a triradiate shape, with apices anchored by intermediate-filament-containing marginal cells and muscle cells on each of the three sides. Contraction of the muscles pulls the lumen open. We do not know the shape of the open lumen, but have assumed an equilateral triangle for simplicity (Fully open). (Note that the size of the lumen is exaggerated for clarity.) In this configuration particles are free to move with the fluid. As the muscles relax the lumen closes. At the point where the diameter of the lumen (defined as the diameter of an inscribed circle) equals the diameter of a particle contained within it, we assume that the particle is held by the walls and no longer moves (Partly open). Liquid can still flow through the three radii. As relaxation continues the particle remains immobile and the walls deform around it (Closed).

Anterior isthmus delay produces inefficient transport

The pharyngeal muscles were assumed to move as summarized in Fig. 5; timing was based on the series of images from which Fig. 3 was abstracted. The corpus begins contracting at time 0, reaches full contraction at 133 ms, and requires 17 ms to relax. Between 0 and 133 ms and between 133 and 150 ms motions are linear, for simplicity. The anterior end of the isthmus contracts from 83 to 150 ms and relaxes from 150 to 167 ms; the middle of the isthmus contracts from 150 to 183 ms and relaxes from 183 to 200 ms. Between the anterior and middle isthmus, times of contraction and relaxation vary linearly with position. The posterior half of the isthmus remains closed through the pump. It was not included in the simulation, so transported particles accumulate in mid-isthmus in the simulation. In reality particles that reach mid-isthmus would eventually be carried back to the terminal bulb by a subsequent posterior isthmus peristalsis.

Fig. 6A–D shows the simulated motion of three particles

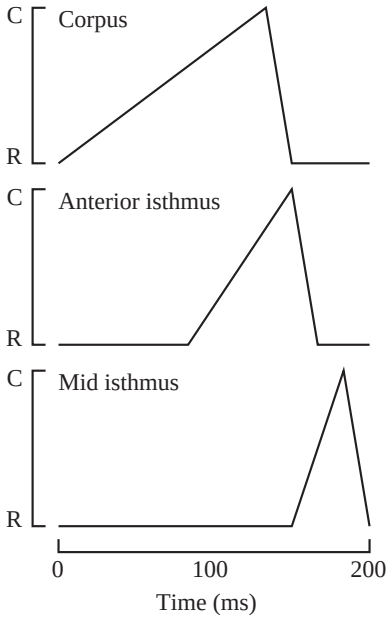

Fig. 5. Summary of corpus and isthmus motions. For simulation, muscle motions were assumed to be piecewise linear as diagrammed here (i.e. the extent of contraction varies linearly with time, except at discrete breakpoints where its rate of change with time abruptly changes.) The corpus contracts from 0 to 133 ms and relaxes from 133 to 150 ms. C indicates the fully contracted position and R the fully relaxed position. The entire corpus contracts and relaxes as a unit. The anterior isthmus contracts from 83 to 150 ms and relaxes from 150 to 167 ms; the middle of the isthmus (the most posterior region included in the simulation) contracts from 150 to 183 ms and relaxes from 183 to 200 ms. Between the anterior and middle isthmus the times at which contraction starts, relaxation starts, and relaxation ends vary linearly. These times are based on the video sequence from which Fig. 3 was abstracted, but the precise times of pharyngeal motions are quite variable. Important features consistently seen are the delay of isthmus motions with respect to the corpus, and the progression of motion from the anterior to the middle isthmus.

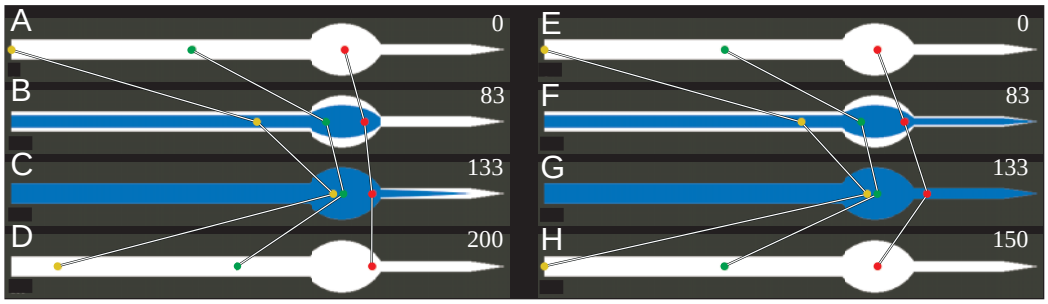

Fig. 6. Simulated particle motions in the pharyngeal lumen. Simulated motions of three particles in the corpus and anterior isthmus. Anterior is to the left; the posterior end of each diagram (the pointed end) represents the middle of the isthmus. (The posterior half of the isthmus and the terminal bulb were not included in the simulation and are not pictured here.) The white region is the maximum possible opening of the lumen, and blue represents the opening at any particular point in time. Time in ms is given in the upper right corner of each panel. (A–D) Motions were simulated as shown in Fig. 5. (E–H) The isthmus was assumed to move in synchrony with the corpus, so that muscle motions are precisely reciprocal. (B,F) (83 ms) The beginning of anterior isthmus contraction, when the corpus is partly contracted; (C,G) (133 ms) maximum corpus contraction, and (D,H) the end of a full cycle. (Because the isthmus motions are not delayed in E–H, the cycle is only 150 ms long.) In A–D, each particle has a slightly more posterior position at the end of the cycle than at the beginning, i.e. there is net transport. In E–H, particles end up precisely where they began, showing that net transport requires the delayed isthmus motions shown in A–D.

placed at the mouth, the middle of the procorpus, and the middle of the metacorpus. For comparison, Fig. 6E–H shows the movement of the same particles if the isthmus had contracted in synchrony with the corpus. As predicted, under these conditions there was no net particle movement; the particles returned to their starting positions (Fig. 6E–H). However, when the isthmus contraction was delayed, all particles finished slightly more posterior than they began (Fig. 6A–D). In fact, repetitive pumping would carry a particle from the mouth to the mid-isthmus. Fig. 7 shows the positions of a particle placed at the mouth after 1, 2, …, 14 pumps. The 14th pump carried it into the isthmus. From here it would be carried to the middle of the isthmus by subsequent pumps; in a real pharynx it would eventually be swallowed.

Simulation reveals the existence of a point of no return. This is most clearly seen by looking at the most posterior particle (the red one) during corpus relaxation (Fig. 6C,D), which does not move. It is located at a stasis point where there is no flow. The stasis point is a watershed. All the liquid in the corpus lumen must leave it during relaxation, but there are two places it can go. Liquid anterior to the stasis point flows out of the mouth, and liquid posterior to it flows into the isthmus lumen, which is expanding at this time. While it lasts, the stasis point is a boundary that nothing can cross. The stasis point exists only during corpus relaxation; during contraction, flow is uniformly posterior. Thus a particle that moves posteriorly past this point during contraction can never cross it again. Any particle that reaches the point of no return will inevitably be carried into the isthmus and eventually swallowed.

The stasis point can also be thought of as the fulcrum of a lever. A particle at the stasis point remains stationary. A particle slightly posterior or anterior to the stasis point moves away from it at a rate and to a final distance that is roughly proportional to the particle's initial distance from it, just as the movement of a lever is proportional to distance from the fulcrum. This leverage explains how net transport is effected. During contraction, particles in the corpus are drawn back toward the middle of the isthmus, but during relaxation, they

Fig. 7. Successive positions of a particle during repetitive pumping, showing its position at the beginning of each of 15 successive cycles. The particle was placed at the mouth (left) at the beginning of the first cycle. The 14th cycle carried it into the isthmus. In the anterior metacorpus some of the pictures of the particle are displaced vertically so that each successive position can be clearly seen, but this is not meant to imply an off-center position.

are pushed away from the stasis point. Because a particle in the corpus is always closer to the stasis point than to the middle of the isthmus, its anterior motion during relaxation is less than its posterior motion during contraction.

Centered particles are transported efficiently

Particles within the relaxed pharynx are consistently located on the center line of the pharyngeal lumen (see, e.g. Fig. 2). This can be explained by the triradiate shape of the pharyngeal lumen, which would squeeze off-center particles to the center as the lumen closes (Fig. 8). A symmetrical contraction of the pharyngeal muscles would be expected to release the particle in the center of the lumen when it opens. Centered particles should move differently from randomly located particles. A randomly located particle will on the average move at the mean fluid velocity, as assumed in the simulation above. However, fluid in the center of a tube moves faster than fluid at the edges because the latter is slowed by friction with the walls. In a tube with the triradiate shape of the pharyngeal lumen, fluid at the center moves from 2.2 times faster than the mean flow velocity for a fully open lumen to 3.5 times when the lumen is nearly closed (see Appendix). As this acceleration will occur for both anterior and posteriorward movement, it is not immediately obvious what effect it will have on net particle transport.

We repeated the simulation, but instead of assuming that particles moved at the mean flow velocity, allowed them to move at the center flow velocity. In addition, to roughly

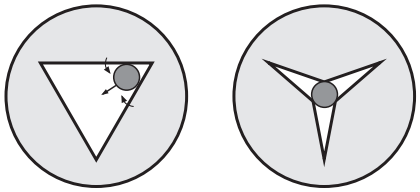

Fig. 8. Particles are pushed to the center of the closing pharyngeal lumen. This figure diagrams how we believe the shape and motions of the pharyngeal lumen during relaxation would push particles to the center. See text for further explanation.

simulate the effect of a partially effective centering mechanism, we simulated the motion of particles moving at a constant factor times the mean flow velocity, with the constant ranging from 1.0 (i.e. mean flow velocity) to 2.0 (slightly less than the slowest expected for a perfectly centered particle). Fig. 9 shows the location of single particles placed at the mouth at time zero after a single contraction–relaxation cycle.

Centered particles are transported far more effectively than particles moving at mean flow velocity. A centered particle is transported the entire length of the procorpus in a single pump (Fig. 9, blue particle). Only two cycles are needed to transport it to the isthmus, compared to 14 for a particle moving at mean fluid velocity. Even small accelerations produce an appreciable effect, and net transport increases more than linearly with velocity. A particle moving at 1.4 times mean flow velocity (Fig. 9, green particle) is transported almost twice as far in the first pump as one moving at mean flow velocity (Fig. 9, brown particle), and enters the isthmus after 8 pumps. A particle moving at twice mean flow velocity (Fig. 9, red particle) is transported more than half the length of the procorpus in the first pump, and enters the isthmus on the fourth.

Net transport of a centered particle, like transport of a particle moving at mean flow velocity, is absolutely dependent on delayed isthmus motions. If the corpus and isthmus contract together (as in Fig. 6E–H) a centered particle is pulled deep into the isthmus during contraction. But because the acceleration operates during anteriorward as well as posteriorward motion, it is transported back to its starting position during relaxation. Thus, the acceleration that results from centering particles does not in itself effect net transport. It merely magnifies the transport produced by delayed isthmus motion.

A simplified model: the four-stage pharynx

The essential features of transport within the corpus can be understood using a simpler model shown in Fig. 10: the four-stage pharynx. In this model the isthmus and corpus are each uniform in diameter along their entire lengths, and each contracts and relaxes as a unit. Furthermore, their motions do not overlap: the corpus contracts (Fig. 10A–C), then the isthmus contracts (Fig. 10C,D), then the corpus relaxes (Fig. 10D-F), then the isthmus relaxes (Fig. 10F,G). Consider the motion of a particle located at the mouth when corpus contraction begins. At first, until the corpus diameter reaches

Fig. 9. Centered particles are transported more efficiently. Four simulations were run in which we measured the final position after a single cycle of a single particle placed at the mouth at time zero. The brown particle was assumed to move at mean fluid velocity as in previous simulations. The green and red particles move at 1.4 and 2.0 times mean fluid velocity, respectively, and the blue particle moves at the calculated velocity of the fluid at the center of the lumen, which varies from 2.2 to 3.5 times mean velocity depending on how open the lumen is at a particular moment. See text for further explanation.

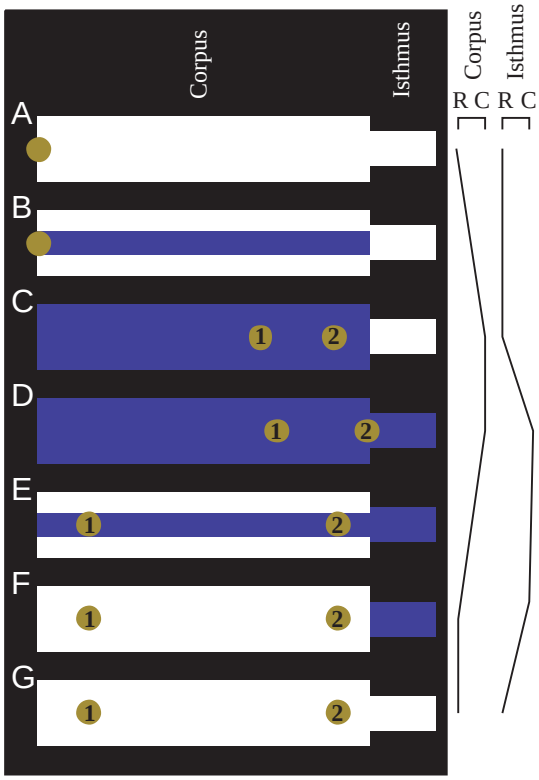

Fig. 10. The four-stage pharynx: a simple model, which captures the essence of our proposed mechanism for particle transport in the corpus. It is so named because the motions occur in four non-overlapping stages: corpus contraction, anterior isthmus contraction, corpus relaxation and anterior isthmus relaxation. (The *contractions* of the isthmus and corpus overlap, in the sense that both are often contracted at the same time, but the *motions* do not overlap: when one is moving, the other holds its position.) Additionally, the corpus and isthmus are each uniform in diameter and motion along their entire lengths. In this figure the movement of a particle placed at the mouth at the beginning of a cycle is followed, and the results are shown for the particle moving at mean fluid velocity (particle 1) or at twice mean fluid velocity (particle 2). The particle has a diameter 1/3 that of the maximum corpus diameter, and the volume of the anterior isthmus is 5% that of the corpus. (B,E) Snapshots taken when the corpus is 1/3 open; it is at these points that the particles become free to move (B) or stop moving (E), because they are held by the walls of the corpus lumen.

the particle diameter, the particle will remain at the mouth, held by the walls of the corpus lumen. When the corpus opens to the particle diameter (Fig. 10B), the particle will be free to move, and will be sucked backward into the corpus (Fig. 10C). Next, the isthmus contracts, and more liquid is sucked in at the mouth and flows through the corpus to fill the isthmus (Fig. 10D). The particle will move backward a small amount. In the third stroke, the corpus relaxes. Liquid flows anteriorly, and at first, for as long as the diameter of the corpus lumen exceeds the particle diameter, the particle moves with the fluid. But when the lumen diameter equals the particle diameter (Fig. 10E), the particle is trapped within the corpus. Because of the triradiate shape of the pharyngeal lumen (Fig. 4), liquid can still flow around the particle. The particle remains where it is while the corpus finishes its relaxation (Fig. 10F) and the isthmus relaxes (Fig. 10G). Like the more realistic simulation, the four-stage pharynx has a point of no return: the boundary between isthmus and corpus. A particle that moves posterior to this point during contraction can never cross it again. (The four-stage model does not correctly reproduce transport within the isthmus: subsequent pumps will produce no net movement of a particle posterior to the corpus/isthmus boundary.)

The four-stage pharynx can be solved exactly. For instance, a particle whose velocity is a times the mean fluid velocity moves distance Δx from the mouth in a single contraction–relaxation cycle:

$$\Delta x = a\left(\frac{D}{d}\right)^{a}\left(\frac{V_{\text{isthmus}}}{V_{\text{corpus}}}\right) l_{\text{corpus}}, \qquad (1)$$

where D is the maximum diameter of the open corpus lumen, d is the diameter of the particle, V_{isthmus} is the volume of fully open isthmus lumen, V_{corpus} is the volume of fully open corpus lumen, and l_{corpus} is the length of the corpus. Equation 1 is valid only for values of $d < D$, i.e. the particle must fit in the corpus lumen, and $\Delta x \leq l_{\text{corpus}}$, i.e. the particle does not reach the isthmus. Although this equation will not produce accurate numbers for the complex geometry of the real pharynx, it is useful as a summary of the parameters that determine how effective transport is. Transport is more effective when the ratio of isthmus volume to corpus volume is large, when the particle is small compared to the corpus diameter, and especially when the particle moves faster than mean fluid velocity.

As in the more realistic simulation, particle velocity has a more than linear effect. For instance, doubling particle velocity (from a=1 to a=2) increases sixfold the distance that a particle of 1/3 corpus diameter is transported. This nonlinear effect results because a fast-moving particle approaches the point of no return between the corpus and the isthmus more closely during contraction than a slow-moving particle does. During corpus contraction, a particle moving at twice the mean flow velocity moves to a point more posterior than one moving at mean flow velocity (Fig. 10A–C). Isthmus contraction pulls it further posterior, double the distance that a particle moving at mean flow velocity moves in the same step (Fig. 10C,D). However, during corpus relaxation, the particle is pushed forward only by the relaxation between it and the point of no return (Fig. 10D–F). A faster-moving particle, because it comes closer to the point of no return during contraction, moves less during relaxation.

Tests of simulation

Effect of relaxation timing

The timing of muscle relaxation seems to be critical for efficient transport. The M3s are a pair of inhibitory motor neurons that innervate corpus muscles. When they fire, they cause inhibitory postsynaptic potentials in pharyngeal muscle, which can end the action potential, thereby causing muscle relaxation (Avery, 1993b; Dent et al., 1997). When the M3s are killed along with all pharyngeal neurons except the two main excitatory types MC and M4, relaxation is delayed and bacteria are inefficiently transported. However, if all pharyngeal neurons except MC, M4 and M3 are killed, relaxation is not delayed and transport is efficient (Avery, 1993b; Avery and Horvitz, 1989). These results suggest that delayed relaxation of pharyngeal muscle results in inefficient transport. We have described mutant strains in which bacterial transport is inefficient (Avery, 1993a). Several of these mutations affect G-protein signaling, and may also affect the action or effectiveness of the M3s (Niacaris and Avery, 2002; Robatzek et al., 2001).

We suspected that these manipulations caused poor transport because they affected the *relative* timing of corpus and isthmus relaxation. To test whether the model could explain the importance of relaxation timing in this way, we simulated transport, holding isthmus motions constant but varying the timing of corpus relaxation, and measured the distance a centered particle placed at the mouth moved. Fig. 11 shows that corpus relaxation time is indeed critical, with transport maximal in a narrow window from 133 to 167 ms. Furthermore, the normal timing measured from video sequences produces near maximal transport.

Effect of particle size

Both the four-stage model and the simulation predict that particles that are small compared to the corpus lumen diameter will be transported more efficiently. Several observations suggest that the size of the pharynx is indeed important for effective feeding. The time immediately after hatching, when the pharynx is at its smallest, is critical for many feeding-impaired mutants. These mutants often fail to grow after hatching and may arrest for days, but once they pass the first larval stage they grow rapidly and become fairly normal adults. This L1 arrest is probably caused by a failure to ingest, because it can be relieved by changing the food (data not shown). Although the pharynx is at its smallest in absolute terms in the newly hatched larva, it is large compared to the worm itself, occupying 29.6±1.3% of the length (71.6±1.0 μm for the pharynx, 242±10 μm for the worm; see Table 1). The pharynx grows rapidly during the first larval stage, but thereafter more slowly than the rest of the animal (J. Hodgkin, personal communication), so that in the adult hermaphrodite it occupies

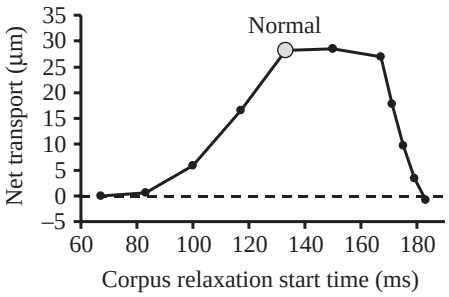

Fig. 11. Relaxation timing affects transport. Summary of a series of simulations in which the timing of corpus relaxation was varied from the base values in Fig. 5 while isthmus motions were held constant, and the transport of a particle placed at the mouth at time zero moving at center fluid velocity was measured. (Negative net transport means that a particle placed within the corpus at time zero was transported anteriorly that distance toward the mouth.) The point labeled 'normal' corresponds to the movement in Fig. 5 and to the blue particle in Fig. 9. For earlier than normal relaxation time, the corpus contracted linearly from time zero to the time plotted on the *x* axis. For later than normal relaxation time, the corpus contracted linearly from 0 to 133 ms, remained contracted until the time plotted, then relaxed. (We also did a series of simulations in which the corpus contracted linearly from time zero to the beginning of relaxation with no pause in the fully contracted state. The results are similar except that the steep fall-off in transport begins at 167 ms instead of 171 ms and is more severe.) Relaxation always took 1/60 s. In this series, anterior isthmus contraction always began at 150 ms. This graph can however be used to predict the results of simulations in which isthmus contraction began at other times by scaling the *x*-axis. For instance, if corpus relaxation began at 120 ms and isthmus relaxation began at 180 ms, net transport would be the same as if corpus relaxation began at 100 ms and isthmus relaxation at 150 ms (5.9 μm from the graph), since (120, 180) can be obtained by multiplying (100, 150) by 1.2. For this statement to be exactly true, all other times, e.g. the time at which mid-isthmus relaxation begins, would also have to be multiplied by 1.2.

only 14.4±0.4% of the length (144.7±0.9 μm/1002±28 μm; Table 1). The increase in diameter is greater than the increase in length. For example, the diameter of the isthmus increases almost fourfold from 4.0±0.1 μm in the newly hatched larva to 15.3±0.3 μm in the adult (Table 1). The large relative size of the pharynx at hatching and its early growth may be caused by selection for attainment of efficient size as early as possible. These observations all suggest that a small pharynx functions poorly compared to a large one.

To test whether food particle size is important we isolated several bacteria from soil and measured how well wild-type and various feeding-defective mutants grew on them. Food is not limiting for wild-type growth on good food sources; feeding-defective mutants allow improved discrimination. Fig. 12 shows the results. Bacterial strains are shown in order of decreasing ability to support growth. As predicted, cell size increases as edibility decreases. The least edible bacteria, in addition to being large in size, form spores (refractile cells in photographs). However, we do not believe that spores are poor at supporting growth, because a spontaneous sporulation-defective mutant of *Bacillus megaterium* L10 is even worse at supporting growth than the parent strain. Furthermore, the correlation between size and edibility is better than between sporulation and edibility. For instance, *Bacillus simplex*, which makes small spores, supports growth about as well as *Pantoea dispersa*, a bacterium of about the same size that was not seen to form spores.

There is one conspicuous exception to the inverse correlation between size and edibility: *E. coli* strain DA837. It is the same size as *E. coli* HB101 but a far worse food source. A lawn of DA837 on a plate of worm medium has a sticky, tacky texture that can be felt with a platinum pick. In contrast, lawns of the other bacterial strains in Fig. 12, including *E. coli* HB101, did not detectably resist the passage of a pick through the bacteria. When bacteria of these strains taken from a worm medium plate are suspended in liquid, they move as individual cells that do not adhere to each other. In contrast, DA837 bacteria are seen in clumps of several cells. (Unfortunately this difference is obvious only when bacteria are suspended free in liquid, and Brownian motion makes it difficult to photograph.) It may be that worms eating DA837 must deal with them as clumps of cells rather than single cells, and that the effective particle size is therefore larger. Alternatively, DA837 may be handled poorly by the pharynx at some step other than transport. This is suggested by the differential effect of worm genotype on ability to grow on DA837: *eat-5* worms are particularly affected. The main effect of *eat-5* is to slow down terminal bulb contractions, with little effect on the corpus.

Discussion

Corpus and isthmus muscle motions

Our principle new observation is that the motions of the muscles of the anterior half of the isthmus occur slightly after those of the corpus during *C. elegans* pharyngeal pumping. In general, anterior to posterior progressing motions of a tubular muscle (such as, for instance, the motions of vertebrate intestinal muscles) will tend to transport lumen contents in the same direction. Thus, it is not surprising that a motion sequence in which the anterior of the pharynx contracts and relaxes before the middle tends to transport particles from anterior to posterior. However, while the observation is clear, there is a problem with the explanation of particle transport it suggests: the isthmus is much smaller than the corpus. We estimate that the volume of the fully open anterior isthmus lumen is less than 5% that of the fully open corpus lumen. The observation that bacteria are always located at the center of the relaxed pharynx suggested a possible way to rescue the mechanism: if particles remained near the center of the lumen during contraction, they would move faster than the mean fluid velocity.

An alternative transport mechanism could be based on posterior-moving waves of contraction or relaxation along the length of the corpus. Indeed, in a previous analysis of corpus and isthmus motions, Seymour et al. (1983) reported that there

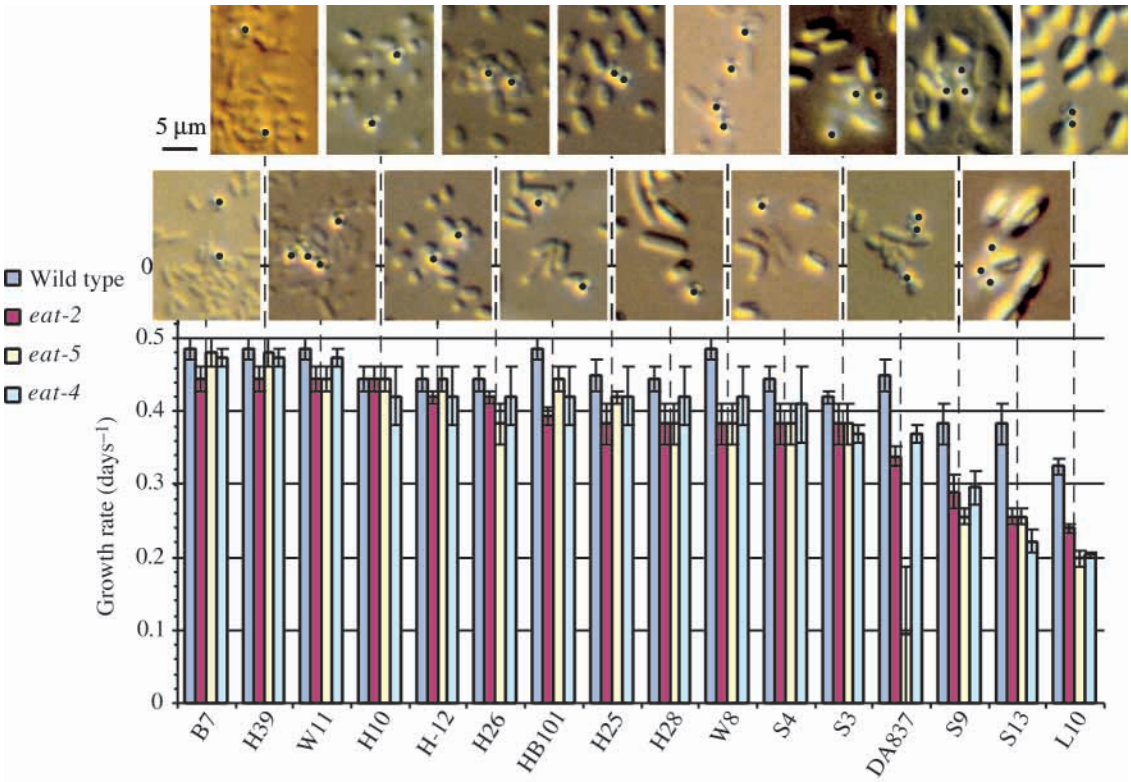

Fig. 12. Effect of bacterial size on edibility. The growth rates (days^{-1}) of wild-type worms and three different feeding-defective mutants on 14 different bacterial strains. The bacteria are listed in order of decreasing *eat-2* growth rate. Above are photographs of each of the bacterial strains as they appear when isolated from lawns on nematode growth medium. The scale bar applies to all pictures. In addition, 0.8 µm blue-dyed latex beads were mixed in with the bacteria as an internal size standard. These are identified by black dots. A strong although not perfect inverse correlation between growth rate and bacterial size is obvious. B7, *Pseudomonas* sp.; H39, *Comamonas* sp.; W11, *Pseudomonas* sp.; H10, Unidentified; H-12, *Acinetobacter junii*; H26, *Pantoea* sp.; HB101, *Escherichia coli*; H25, *Acinetobacter* sp.; H28, *Bacillus simplex*; S4, *Panteoa dispersa*; S3, *Bacillus licheniformis*; DA837, *Escherichia coli*; S9, *Bacillus* sp.; S13, *Bacillus cereus*; L10, *Bacillus megaterium*.

are such waves of motion: '*successive regions of the triradiate oesophageal [i.e. pharyngeal] lumen are opened by their radial muscles, beginning with the procorpus and followed by the metacorpus and isthmus*' and '*As soon as the bacteria reach the mid procorpus the whole oesophageal lumen begins to close from the anterior end backward*'. While such motions would easily explain net particle transport, we have been unable to confirm that they occur. Seymour et al.'s statement was based on 24 frame s^{-1} ciné recordings of *unc-15* and *unc-51* mutant animals, since they were unable to get useful recordings from the more active wild-type animals. We observe that both of these mutants have obviously abnormal feeding behavior: for instance, they pump more slowly than wild type (L. Avery, unpublished observation). Our video recordings, which could be analyzed at a resolution of 1/60 s, were made from wild-type and *unc-29* animals. *unc-29* encodes a body muscle-specific nicotinic acetylcholine receptor subunit (Fleming et al., 1997) and has no effect on pharyngeal muscle motions. In these recordings the corpus appears to open and to close simultaneously along its entire length, and to have perfectly reciprocal motions. We have also looked at a videotape made from Seymour et al.'s ciné recordings, and at a high-speed video recording made by Lars Philipson (personal communication). In none of these recordings could we see any hint that the anterior corpus opens or closes before the posterior. Indeed, in Philipson's high-speed recording it sometimes appeared that the closing of the procorpus began slightly *after* that of the metacorpus, as if the pressure of the fluid being forced out of the metacorpus briefly resisted the closing of the procorpus. This slight delay, if it had an effect, would tend to result in anteriorward particle transport. Thus, we do not believe that transport is effected by waves of corpus muscle motion.

Simulation of particle transport

A pharynx in which motions are perfectly reciprocal and in which particles when free move at mean fluid velocity would clearly not produce net transport. It was intuitively clear that delayed isthmus motions, while they are a deviation in the right direction from reciprocity, would produce at best inefficient transport of particles moving at mean fluid velocity. Without delayed isthmus contraction, there would obviously be no net transport, even of particles that move faster than mean fluid velocity. But unassisted intuition failed to predict how these two deviations from the reciprocal/mean velocity case would interact: would faster particle motion enhance or weaken the

effect of the delayed isthmus contraction, and if so, by how much? To answer this question we found it necessary to simulate fluid and particle motions. Interestingly, particle motion faster than mean velocity powerfully (more than linearly) enhanced the effect of delayed isthmus motions. Furthermore, with the aid of the simulation, it was possible to understand how the two factors interact and the synergism: delayed isthmus motions create a stasis point during corpus relaxation, and accelerated particle motion allows particles to approach more closely or pass this point of no return. With this new intuitive understanding in hand, we developed a simpler model, the four-stage pharynx which, while not geometrically or quantitatively accurate, captures the essentials of transport in an easily understandable way.

In our model particle motion is determined by three assumptions. (1) When the diameter of the pharyngeal lumen is smaller than the particle diameter, the particle is unable to move. (2) When the diameter of the pharyngeal lumen is greater than the particle diameter, particles are free to move and move with the fluid. (3) Particles are located at the center of the pharynx and move at the center flow velocity.

Assumptions 1 and 2 are intuitively plausible and consistent with observation (e.g. Fig. 2). Assumption 3, the most important novelty of the proposed mechanism, is hypothetical and cannot easily be verified by observation. Indeed, it is certainly not exactly true; with time some displacement from the center is inevitable (and is indeed visible in Fig. 2G). However, several arguments suggest that faster motion at the center is likely to contribute to particle transport. First, bacteria are consistently located at the center of the relaxed pharynx, as shown for instance in Fig. 2I. As the pharynx begins to contract, a particle must remain near the center during the time period immediately after it is released, because it will simply not fit anywhere else. This period is the most important for transport, because the cross-sectional area of the lumen is small, meaning higher fluid velocity for a given flow rate. As the contraction proceeds, a particle may tend to leave the precise center of the lumen, but as long as it remains away from the walls it will move faster than the mean flow velocity, and our simulation shows that even a small acceleration improves transport (Fig. 9). Moreover, diffusion of a particle away from the center will not necessarily make transport worse: if the particle is approximately centered during contraction but off-center during relaxation it will move more rapidly posteriorly than it does anteriorly, resulting in even greater net transport.

Every application of mathematics to the real world requires approximations. In this simulation the approximations are many, including the following. (1) Interaction of particles was not modeled. (2) Free particles were assumed to move at center fluid velocity. In reality, they would move slower because of their finite size, and because they would tend to be pushed away from the center by Brownian motion and less than perfectly symmetric muscle motions. (3) The pharyngeal lumen was assumed to have a simple triradiate shape (Fig. 4); the real cross-section, however, is more complex and varies along the length of the pharynx (Albertson and Thomson, 1976). (4) The diameter of the lumen as a function of position along the pharynx is more complex in reality than in the model. (5) Muscle motions were assumed to be piecewise linear functions of time (Fig. 5). Assumption 1 was made for computational convenience and because it represents an important limiting case, but assumptions 2–5 were necessary because of lack of information, since we do not have the data to replace these assumptions with more realistic parameters. (Also, the shape and motions of the pharynx vary with age and environment, leading us to suspect that some of these quantitative details might not matter greatly.) For these reasons, we cannot claim that the simulation models particle transport in a quantitatively accurate way (although it may). We feel, however, that it probably captures the key qualitative features of transport, for two reasons. First, as described above, its workings are intuitively understandable in a way that does not depend on the suspect quantitative details of motion or geometry. Second, it resembles the real pharynx, both in the efficiency with which it transports particles, and in the effect of certain perturbations on transport.

The power of the model is shown by its ability to explain a past observation and to make a new prediction. The past observation is that the timing of corpus relaxation is important for effective particle transport. Intuitively our model explains this because corpus motions must occur before isthmus motions for transport to occur. Simulation shows in fact that timing does matter, and that the actual muscle motions measured from videotape are near-optimal (Fig. 11). The new prediction is that smaller particles will be transported more effectively, and therefore that there will be an inverse correlation between bacterial size and ability to sustain *C elegans* growth. This is not an intuitively obvious prediction: while it is clear that bacteria must fit in the pharynx to be transported, it is not obvious without understanding the mechanism why a large particle that fits in the lumen will be transported less well than a small one. Indeed, in more conventional filter-feeding systems, larger particles are more easily separated from fluid than small ones. However, it was borne out by measurements of growth on different soil bacteria isolates (Fig. 12).

Particle trapping versus particle transport

Although we have focused on particle transport, the model we propose is also capable of trapping particles. With simulation parameters based on experimental measurements, bacteria that enter the mouth within 58 ms of the beginning of corpus contraction are trapped within the corpus. Bacteria that enter after 58 ms are expelled during corpus relaxation. However, it is virtually certain that the simulation does not trap particles in the same way as the real pharynx. First, trapping seems to be more effective in the real pharynx; particles that enter the pharynx are rarely seen to leave again. Second, Seymour et al. (1983) reported (and we have confirmed) that bacteria usually do not enter the corpus until near the end of the contraction, precisely the time at which they would be least effectively trapped in the simulation. Normally the metastomal flaps at the anterior end of the pharynx block bacteria from

entering during most of the corpus contraction; instead, they pile up in the buccal cavity, a sort of vestibule to the pharynx. Just before corpus relaxation the metastomal flaps move, allowing the bacteria to enter the corpus lumen, where they are trapped by a mechanism that remains mysterious. It seems likely that the metastomal flaps and the small pm1 and pm2 muscles that operate them are somehow involved, but because of their small size and the rapidity of the events, we have been unable to see how they operate.

Conclusion

Our results do not establish the mechanism of particle transport in the *C. elegans* pharynx. Direct confirmation would require high-speed video recordings of bacteria-sized particles moving in the lumen of the pharynx during pumping, which is technically difficult. We can say, however, that no exotic mechanisms are required to explain particle transport. By combining the observed muscle motions with three assumptions, two of them not controversial and one plausible though unproven, we can reproduce in simulation the efficient transport observed in the animal.

Appendix

Simulation of the anterior pharynx

Pharyngeal geometry

For simulation, the pharynx from the middle of the isthmus to the anterior end was modeled as a series of sections, each with a characteristic maximum cross-sectional area A_{max} and length l, both independent of time. l is the length of the section along the anterior–posterior axis. At any given time the section may be closed, partially open, or fully open. A, the cross-sectional area of the lumen, varies between 0, when the lumen is closed, to A_{max}, when the lumen is fully open. The opening O of the section, defined as A/A_{max}, thus varies between 0 and 1.

O is the parameter used to describe pharyngeal motions, and is plotted in Fig. 5. A and O vary with time, but are invariant along the length of a section. The volume of a section is $lA=lA_{max}O$. The four-stage pharynx consists of just two sections: corpus and isthmus. In the more realistic simulation, the entire procorpus was modeled as one section, since it was assumed to be constant in diameter and to move as a unit. The isthmus, although constant in diameter along most of its length, was modeled as a series of small sections of length $l\approx57$ nm, because the timing of its motions varied along the length, and the metacorpus was also modeled as a series of small sections since it varies in diameter. x, position along the anterior–posterior axis, was set to 0 at the middle of the isthmus, and increased in the anterior direction. This the posteriormost section, section 1, extends from $x=0$ to $x=l_1$, the next most posterior section from $x=l_1$ to $x=l_1+l_2$, etc.

To simulate the movement of a particle of finite size, it was necessary to calculate the radius of the largest circle that can be inscribed in the lumen at a given O, so that we could determine when the particle was held by the walls and when free to move. This required that we choose a particular geometry for the pharyngeal lumen. We assumed that the lumen varied between a Y-shaped structure when fully closed to an equilateral triangle when fully open (Fig. 4). We also assumed that the apices of the lumen did not move. [This is unlikely; the apices probably move away from the center somewhat as the pharynx contracts. However, we did not have the data to model this more accurately, and in any case it has little effect on the simulation; it simply means that the true value of O at which a particle will be caught is slightly smaller than the one we used, i.e. our approximation is effectively the same as making the particle slightly bigger. This assumption also affects the calculation of center fluid velocity as a function of O (see below), but since the ratio of center to mean velocity varies only slowly with O, this should have little effect.]

r_{max} is the radius of a circle inscribed in the lumen open to its maximum extent, when it is assumed to have an equilateral triangle cross-section. Equivalently, r_{max} is the distance from the center of the fully open pharyngeal lumen to any of the three closest points on the lumen wall (Fig. 13).

$$A_{max} = 3\sqrt{3r_{max}^2}. \tag{2}$$

$r(O)$, the radius a circle inscribed in the lumen at opening O, is then just:

$$r = Or_{max}. \tag{3}$$

Fluid and particle motions

Because we assumed the posterior isthmus to remain closed, the lumen had to fill and empty through the mouth. Flow ϕ through the mouth is therefore just the rate of change of the volume of the pharyngeal lumen. Flow through a cross-section at position x is equal to the rate of change of the volume of the lumen posterior to x. In particular, flow through the anterior boundary of section n is equal to the sum of the rates of change of volume of sections 1 through n:

$$\phi_{an} = \phi_{p,n+1} = \sum_{i=1}^{n} \dot{V}_i = \sum_{i=1}^{n} l_i\dot{A}_i = \sum_{i=1}^{n} l_i A_{max,i}\dot{O}_i. \tag{4}$$

($\dot{O}\equiv dO/dt$, $\dot{A}\equiv dA/dt=A_{max}\dot{O}$, $\dot{V}\equiv dV/dt=l\dot{A}$ and $\phi_{p,n+1}$ represents flow through the posterior boundary of section n+1.) We represented O as a function of time as piecewise linear functions (Fig. 5): that is, O varies linearly with time except at discrete breakpoints where its rate of change with time abruptly changes. Thus, $\dot{O}_i$ and $\dot{A}_i$ are constant between breakpoints of section i. ϕ_{an} changes at breakpoints of section n or any section posterior to it.

For x within a section extending from x_p to $x_a=x_p+l$, ϕ is linear with x:

$$\phi x = \phi_p + (\phi_a - \phi_p)\frac{(x-x_p)}{(x_a-x_p)} = \phi_p + \dot{A}(x-x_p). \tag{5}$$

Mean flow velocity v at x is:

$$v(x) = \phi(x)/A = \frac{1}{O}\left(\frac{\phi_p}{A_{max}} + \dot{O}(x-x_p)\right). \tag{6}$$

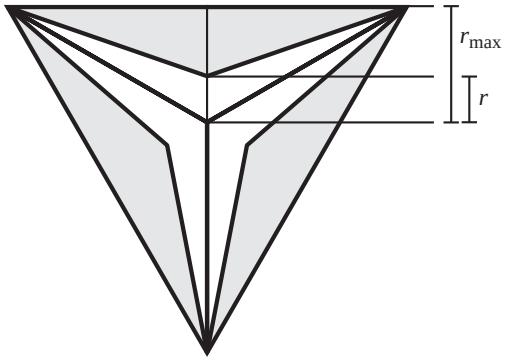

Fig. 13. Parametrization of pharyngeal lumen opening, showing how the parameters r and r_{max} were defined. The white area represents a cross-section of the lumen open to radius r, and the tinted area the maximum possible opening r_{max} for this cross-section.

A particle moving at mean flow velocity follows the differential equation:

$$\frac{dx}{dt} = -v(x), \tag{7}$$

which can be solved to give:

$$x(t) = \frac{A_{max}O_0x_0 + tA_{max}x_p\dot{O} - t\phi_p}{A_{max}O_o + tA_{max}\dot{O}} = \frac{1}{A(t)}(A_0x_0 + tx_p\dot{A} - t\phi_p), \tag{8}$$

where A_0, O_0 and x_0 are the values of A, O and x at time 0. This solution is valid until the particle moves out of the section, until a breakpoint of the section changes $\dot{A}$, or until a breakpoint of a section posterior to it changes ϕ_p. This equation can be solved for t to predict the time at which a particle will reach a particular location x:

$$t(x) = \frac{A_{max}O_0(x_0 - x)}{A_{max}\dot{O}(x - x_p) + \phi_p} = \frac{A_0(x_0 - x)}{\phi(x)}. \tag{9}$$

This solution has a simple intuitive interpretation: $A_0(x_0–x)$ is the volume of fluid between x and x_0 at time 0; t is just the time it takes for that amount of fluid to flow past x.

An important special case occurs when $\phi(x)$ and ϕ_p are opposite in sign. For instance, consider a section into which liquid is flowing at both the anterior and posterior ends. This requires that the pharynx posterior to the section be relaxing and expelling liquid, so that ϕ_p is negative, and that the section be contracting, so that $\dot{V}>–\phi_p$, making $\phi_a=\dot{V}+\phi_p>0$. If we try to use Equation 9 to calculate when a particle that begins at x_p will reach x_a, we get $t=–A_0l/\phi_a$, a negative number. But since the particle is moving in the anterior direction, toward x_a, this answer cannot be correct. In fact, the particle will never reach x_a. There is a watershed or stasis point within the section at $x=x_a–\phi_a/(\phi_a–\phi_p)$ where $\phi(x)=0$. Nothing can cross this boundary. It is such a stasis point that leads to the point of no return in the posterior metacorpus that is so important to understanding how the model transports bacteria. This special case also occurs for accelerated particles and centered particles (below).

Simulation method

Motions of particles, fluid and the pharyngeal lumen were simulated by a discrete event method. Between events we used Equation 8 to calculate the movement of particles moving at mean fluid velocity. An ‘event’ is any discontinuity at which the equation becomes invalid or at which its parameters change. The most important events are the release of a caught particle by the contracting pharyngeal lumen, the catching of a free particle by the relaxing lumen, motion breakpoints of the section the particle is currently in or any posterior section, and the movement of the particle into an adjacent section. The times of all these events can be predicted: the first three from particle size and the predetermined pharyngeal motions, and the last from Equation 9. The simulation was projected forward to the earliest of them, and Equation 8 was used to calculate particle position at the time of the event. Event times were then recalculated and the simulation projected forward to the next event, etc. Because positions were calculated from analytical solutions to the differential equations governing motion, time is effectively continuous. That is, we did not approximate time as a series of discrete steps during which motions followed simplified approximations, as is necessary when differential equations are solved numerically. Similarly, particles move in a continuous space, although a discrete spatial approximation was introduced in modeling the pharynx as a series of sections.

In addition to the four events at which motions change, we also defined ‘snapshot’ events: these were predetermined time points at which all particle positions and lumen diameters were calculated for use in drawing images like those shown in Figs 6 and 7. Yet another event type was used to place new particles at specified positions along the pharynx (most often at the mouth) at specified times. The simulation, written in the java programming language (http://java.sun.com), is available at http://eatworms.swmed.edu/~leon/pharynx_sim/.

Accelerated particles

The motions of a particle whose velocity is the mean fluid velocity multiplied by a constant factor a are solved in a similar manner. Equation 7 becomes:

$$\frac{dx}{dt} = -av(x), \tag{10}$$

and the solutions are:

$$x(t) = \frac{1}{\dot{A}}\left[\dot{A}x_p - \phi_p + \left(\frac{O_0}{O(t)}\right)^a \phi(x_0)\right], \tag{11}$$

$$t(x) = \frac{O_0}{\dot{O}}\left[\left(\frac{\phi(x_0)}{\phi(x)}\right)^{\frac{1}{a}} - 1\right]. \tag{12}$$

Equations 11 and 12 are used to simulate the motion of an accelerated particle in the same way as Equations 8 and 9 were used to simulate the motion of a particle that moves at mean fluid velocity.

Centered particles

A particle that moves at the velocity of fluid in the center of the pharyngeal lumen also follows Equation 10, but a is now a function of O and therefore of time. We used a local Poiseuille flow approximation to determine how flow velocity varied across the cross-section of the lumen. This approximation is valid if inertial forces can be neglected, and if flow is axial or nearly so (i.e. if lumen diameter changes slowly with x). Velocity then follows Poisson's equation:

$$\nabla^2 v(y,z) = \frac{1}{\eta}\frac{dP}{dx}, \tag{13}$$

where η is viscosity and P is pressure, with the boundary condition:

$$v(y,z) = 0, \tag{14}$$

for y, z on the wall. Since we needed only the ratio of center velocity to mean velocity, we solved Equation 13 with the right-hand-side set to 1. (In principle we could determine P from the simulation. However, because of the unrealistic assumption that the lumen closes perfectly, P determined from the simulation would reach much higher values than in reality. Actually, the pharyngeal lumen is so shaped that it does not close perfectly, especially in the anterior procorpus where flow is highest (Albertson and Thomson, 1976). To simulate pressure accurately we would need more data about the shape of the lumen. The pressure is not necessary for calculation of particle and fluid motions.)

Equation 13 was solved numerically by simulated diffusion on a lattice. The method is based on that described by Hunt et al. (1995), but we made one important change. Hunt et al. (1995) calculated the average number of steps that a particle placed in the interior of the lumen takes to reach the wall. We instead counted the average number of times a diffusing particle hit each lattice point. This also solves the finite difference version of Equation 13, but is computationally more efficient since it requires only a simple increment of the hit count at each step. The C source for our program is available at http://eatworms.swmed.edu/Worm_labs/Avery/flowsim/.

The program takes input on the geometry (necessary to specify the boundary condition Equation 14) in raster image files. Using a commercial drawing package (Deneba Canvas), we created 10 images of the pharyngeal lumen for O=0.1, 0.2, …, 1.0 on a 289×250 pixel lattice and solved Poisson's equation for each. We show the solution for O=0.3 in Fig. 14 as an example. At this value of O, a, the ratio of center to mean flow velocity, was 2.95. For the series, a varied from 2.21 at O=1.0. to 3.32 at O=0.1, and was well fit (r^2=0.9993) by the quadratic a=1.0097O^2–2.366O+3.5587. The solution of Equation 10 is:

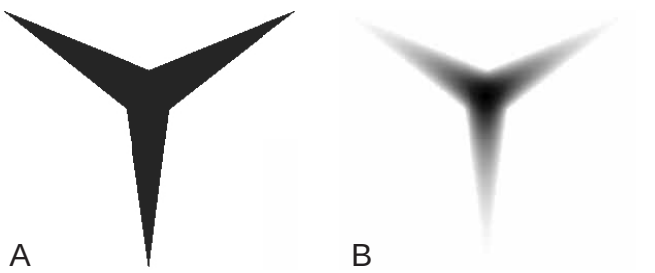

Lumen geometry, O=0.3 Flow velocity (black fastest)

Fig. 14. Calculated flow field in the 30% open pharyngeal lumen. (A) The shape of the pharyngeal lumen at 30% of its maximum opening as a 289×250 pixel image. This image was used directly as input for numerical solution of Poisson's equation (B).

$$x(t) = \frac{O_0^{c_0}(x_0 - x_p)}{\alpha(t)} + x_p + \left(\frac{O_0^{c_0}}{\alpha(t)} - 1\right)\frac{\phi_p}{\dot{A}}, \tag{15}$$

where:

$$\begin{aligned} c_0 &= 3.5587 \\ c_1 &= 2.366 \\ c_2 &= 1.0097 \\ \alpha(t) &= e^{\dot{O}t[c_1 + c_t O(t)]} O(t)^{c_0}. \end{aligned} \tag{16}$$

Equation 15 is used to calculate the motion of a centered particle. We were unable to solve Equation 15 for t. We therefore used an iterative numerical method to calculate the time at which a centered particle would reach a given x:

(1) Calculate a=1.0097O^2–2.366O+3.5587 for time 0.

(2) Use Equation 12 to calculate the time t_1 at which an accelerated particle with acceleration a would reach point x from starting position x_0.

(3) Use Equation 15 to calculate the position x_1 that a centered particle would reach at time t_1. x_1 will be different from x because O will have changed between time 0 and time t_1. However, because a varies only slowly with O, the difference will generally not be large.

(4) Repeat, starting from time t_1 and position x_1 to calculate a new time t_2 and position x_2, then if necessary a time t_3 and position x_3, etc, until an x_i sufficiently close to x is found.

This worked well: even with a tolerance in step 4 of less than a femtometer, it converged in 3 iterations or less. For small distances such as obtain in the isthmus and metacorpus where sections are small, a single iteration was usually enough.

We would like to thank Uday Apte and Ellen Allen for exposing us to simulation software. This work was supported by NIH research grant HL46154 from the US Public Health Service.

References

Albertson, D. G. and Thomson, J. N. (1976). The pharynx of *Caenorhabditis elegans*. *Phil. Trans. R. Soc. Lond. B* **275**, 299-325.

Avery, L. (1993a). The genetics of feeding in *Caenorhabditis elegans*. *Genetics* **133**, 897-917.

Avery, L. (1993b). Motor neuron M3 controls pharyngeal muscle relaxation timing in *Caenorhabditis elegans*. *J. Exp. Biol.* **175**, 283-297.

Avery, L. and Horvitz, H. R. (1987). A cell that dies during wild-type *C. elegans* development can function as a neuron in a *ced-3* mutant. *Cell* **51**, 1071-8.

Avery, L. and Horvitz, H. R. (1989). Pharyngeal pumping continues after laser killing of the pharyngeal nervous system of *C. elegans*. *Neuron* **3**, 473-85.

Avery, L. and Horvitz, H. R. (1990). Effects of starvation and neuroactive drugs on feeding in *Caenorhabditis elegans*. *J. Exp. Zool.* **253**, 263-270.

Davis, M. W., Somerville, D., Lee, R. Y., Lockery, S., Avery, L. and Fambrough, D. M. (1995). Mutations in the *Caenorhabditis elegans* Na,K-ATPase alpha-subunit gene, *eat-6*, disrupt excitable cell function. *J. Neurosci.* **15**, 8408-8418.

Dent, J. A., Davis, M. W. and Avery, L. (1997). *avr-15* encodes a chloride channel subunit that mediates inhibitory glutamatergic neurotransmission and ivermectin sensitivity in *Caenorhabditis elegans*. *EMBO J.* **16**, 5867-5879.

Emmons, S. W., Klass, M. R. and Hirsh, D. (1979). Analysis of the constancy of DNA sequences during development and evolution of the nematode *Caenorhabditis elegans*. *Proc. Natl. Acad. Sci. USA* **76**, 1333-1337.

Fleming, J. T., Squire, M. D., Barnes, T. M., Tornoe, C., Matsuda, K., Ahnn, J., Fire, A., Sulston, J. E., Barnard, E. A., Sattelle, D. B. et al. (1997). *Caenorhabditis elegans* levamisole resistance genes *lev-1*, *unc-29*, and *unc-38* encode functional nicotinic acetylcholine receptor subunits. *J. Neurosci.* **17**, 5843-5857.

Harris, J. and Crofton, H. (1957). Structure and function in the nematodes: Internal pressure and cuticular structure in *Ascaris*. *J. Exp. Biol.* **34**, 116-130.

Hunt, F., Douglas, J. and Bernal, J. (1995). Probabilistic computation of Poiseuille flow velocity fields. *J. Math. Phys.* **36**, 2386-2401.

Lee, R. Y., Sawin, E. R., Chalfie, M., Horvitz, H. R. and Avery, L. (1999). EAT-4, a homolog of a mammalian sodium-dependent inorganic phosphate cotransporter, is necessary for glutamatergic neurotransmission in *Caenorhabditis elegans*. *J. Neurosci.* **19**, 159-167.

Niacaris, T. and Avery, L. (2002). Serotonin regulates repolarization of the *C. elegans* pharyngeal muscle. *J. Exp. Biol.* **206**, 223-231.

Purcell, E. M. (1977). Life at low Reynolds number. *Am. J. Phys.* **45**, 3-11.

Raizen, D. M., Lee, R. Y. and Avery, L. (1995). Interacting genes required for pharyngeal excitation by motor neuron MC in *Caenorhabditis elegans*. *Genetics* **141**, 1365-1382.

Robatzek, M., Niacaris, T., Steger, K., Avery, L. and Thomas, J. H. (2001). *eat-11* encodes GPB-2, a Gbeta(5) ortholog that interacts with G(o)alpha and G(q)alpha to regulate *C. elegans* behavior. *Curr. Biol.* **11**, 288-293.

Seymour, M., Wright, K. and Doncaster, C. (1983). The action of the anterior feeding apparatus of *Caenorhabditis elegans* (Nematoda: Rhabditida). *J. Zool. Lond.* **201**, 527-539.

Sulston, J. E. and Hodgkin, J. A. (1988). Methods. In *The Nematode* Caenorhabditis elegans (ed. W. B. Wood and the Community of *C. elegans* Researchers), pp. 587-606. Cold Spring Harbor: Cold Spring Harbor Laboratory Press.

Vogel, S. (1994). *Life in Moving Fluids: The Physical Biology of Flow*. Princeton, NJ: Princeton University Press.